

# Transport properties of electrons in CF<sub>4</sub>

T. Caldwell<sup>c</sup> A. Roccaro<sup>a,h</sup> T. Sahin<sup>c</sup> H. Yegoryan<sup>c</sup>  
 D. Dujmic<sup>d,\*</sup> S. Ahlen<sup>a</sup> J. Battat<sup>c</sup> P. Fisher<sup>c,d,e</sup> S. Henderson<sup>c</sup>  
 A. Kaboth<sup>c</sup> G. Kohse<sup>f</sup> R. Lanza<sup>g</sup> J. Lopez<sup>c</sup> J. Monroe<sup>c</sup>  
 G. Sciolla<sup>c</sup> N. Skvorodnev<sup>b</sup> H. Tomita<sup>a</sup> R. Vanderspek<sup>c</sup>  
 H. Wellenstein<sup>b</sup> R. Yamamoto<sup>c</sup>

<sup>a</sup>*Physics Department, Boston University, Boston, MA 02215*

<sup>b</sup>*Physics Department, Brandeis University, Waltham, MA 02454*

<sup>c</sup>*Department of Physics, MIT, Cambridge, MA 02139*

<sup>d</sup>*Laboratory for Nuclear Science, MIT, Cambridge, MA 02139*

<sup>e</sup>*MIT Kavli Institute for Astrophysics and Space Research, Cambridge, MA 02139*

<sup>f</sup>*Nuclear Reactor Laboratory, MIT, Cambridge, MA 02139*

<sup>g</sup>*Department of Nuclear Science and Engineering, MIT, Cambridge, MA 02139*

<sup>h</sup> *Deceased*

DMTPC Collaboration

---

## Abstract

Carbon-tetrafluoride (CF<sub>4</sub>) is used as a counting gas in particle detectors, but some of its properties that are of interest for large time-projection chambers are not well known. We measure the mean energy, which is proportional to the diffusion coefficient, and the attenuation coefficient of electron propagation in CF<sub>4</sub> gas using a 10-liter dark matter detector prototype of the DMTPC project.

*Key words:* dark matter, directional detector, CF<sub>4</sub>, carbon-tetrafluoride, TPC, electron diffusion, electron attachment, DMTPC

*PACS:* 29.40.Cs, 29.40.Gx, 95.35.+d

---

\* Corresponding author.

*Email address:* ddujmic@mit.edu (D. Dujmic).

## 1 Introduction

Since carbon tetrafluoride ( $\text{CF}_4$ ) has a wide spectrum of applications, most of its properties are well determined (see e.g. [1]).  $\text{CF}_4$  gas has been suggested as a good target for directional [2], spin-dependent dark matter searches [3,4,5,6] due to the large spin of the fluorine nucleus and the good ionization-counting properties of the molecule. However, there is a large discrepancy between existing measurements of electron transport parameters, specifically the diffusion and attachment coefficients, that are of vital importance for the design of low-background particle detectors such as dark matter searches. Detectors that are based on the time-projection-chamber (TPC) concept [7] require long drift distances of ionization electrons through detector gas in a low electric field. As a swarm of electrons propagates along an electric field, it spreads transversely and longitudinally, which limits spatial precision of the detector. Current measurements of the transverse spread [8,9,10] differ by more than an order of magnitude at operating conditions needed for dark matter detection. Primary electrons can also attach to  $\text{CF}_4$  molecules (see [1] for details), which attenuates the electron signal in the detector. Measurements of the attenuation rate also differ by more than an order of magnitude [11,12]. In this work, we present new measurements of the mean electron energy, that determines the transverse diffusion, and the attenuation coefficient of electrons in  $\text{CF}_4$  gas.

## 2 Experimental setup

The detector (Figure 1) is a low-pressure time projection chamber with optical and charge readout. Particles interacting in the sensitive volume of the detector ionize the gas either directly or by creating a charged particle recoil. The sensitive region of the detector is surrounded by a series of stainless steel rings with inner diameter of 27 cm, outer diameter of 32 cm, and thickness of 1 mm. The rings are connected with 1 M $\Omega$  resistors and separated by nylon washers to keep periodicity at 1 cm. The last ring in the series is connected via a 2.2 M $\Omega$  resistor to a ring holding a grounded mesh and is separated from the mesh by 1.7 cm. The total height of the drift region is 19.7 cm. The field uniformity in the drift cage is computed using the finite element method (FEM) with the scaled transverse field component,  $|E_{\perp}|/|E|$ , less than 1%. The cathode is made of a stainless-steel wire mesh with a pitch of 512  $\mu\text{m}$  and wire diameter of 31  $\mu\text{m}$ . The grounded electrode is made of a stainless-steel mesh with a pitch of 256  $\mu\text{m}$  and wire diameter of 28  $\mu\text{m}$ . The detector consists of two TPCs put back-to-back such that electrons drift toward two amplification planes located in the center of the vessel. Only the top TPC is used in these measurements.

The amplification plane is described in more detail in [13]. An amplification gap is created by a copper anode (+730 V) and a grounded mesh separated with 0.53 mm fishing lines that are placed at 2.5 cm intervals. Primary electrons that drift toward the plane start avalanches of electrons and scintillation photons [14,15]. The detector's primary form of readout is the two-dimensional optical readout of scintillation photons created in the avalanche charge multiplication process. This scintillation light is collected with a Nikon photographic lens with f-stop ratio of 1.2 and a focal length of 55 mm. The scintillation light is recorded by an Apogee U6 camera with a Kodak 1001E CCD chip. In addition to the optical readout, the charge deposited on the anode is also recorded. We use a proportional preamplifier (Ortec 109PC) to integrate the charge signal and a shaping amplifier (Ortec 485) to make unipolar pulses. A fast digitizer (Alazar ATS860) is used to convert pulses into waveforms, which are saved with our event record. The gas pressure is measured by an Inficon

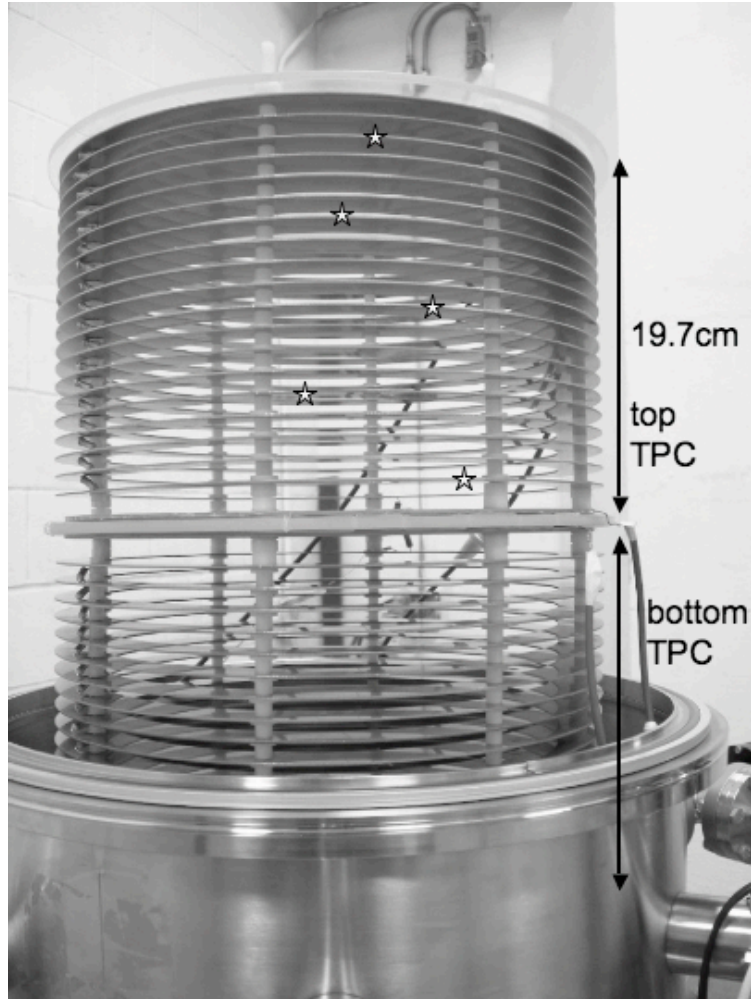


Fig. 1. Drift cages of the 10 liter DMTPC detector with anode planes in the middle. CCD cameras that image light created near anodes are placed above and below the drift cages. The top drift cage is used in measurements. Positions of alpha sources are marked with stars.

PCG400 pressure gauge which utilizes a combination of a capacitance and a Pirani gauge.

The spatial resolution is estimated by extracting the track width of 5.486 MeV alpha particles from an  $^{241}\text{Am}$  source. The observed width of the track along the axis in the readout plane is 300-500  $\mu\text{m}$ . The resolution is affected by the number of CCD pixels,  $n_{bin}$  merged into a readout bin ( $98\mu\text{m} \cdot n_{bin}$ ), the spread of an electron avalanche in the amplification gap ( $\sim 80\mu\text{m}$ ) [16], and the mesh pitch ( $256\mu\text{m}/\sqrt{12} \sim 74\mu\text{m}$ ). The measurement itself is affected by the imperfect collimation of the source (50  $\mu\text{m}$ ) and the straggling of alpha particles through  $\text{CF}_4$  gas (40  $\mu\text{m}$ ) [17] in a 1.2 mm-long track segment. However, the dominant contribution to the spatial resolution uncertainty comes from the electron diffusion that is described and measured in the next section.

We measure the energy resolution at 5.9 keV for the charge readout using a Fe-55 source. A background-subtracted spectrum of pulse heights is fitted with a narrow Gaussian for the full-absorption peak plus a wide Gaussian for the escape peak. The resolution is extracted from the narrower Gaussian and is found to be 10%; a result which is consistent with Fano factor of one [18]. We infer the energy resolution for the CCD readout from the amount of light that alpha particles deposit in track segments of different lengths. The energy deposited into ionization is estimated from the energy loss and calculated by SRIM [17]. We find that the resolution at 55 keV is approximately 15%, as shown in Figure 2.

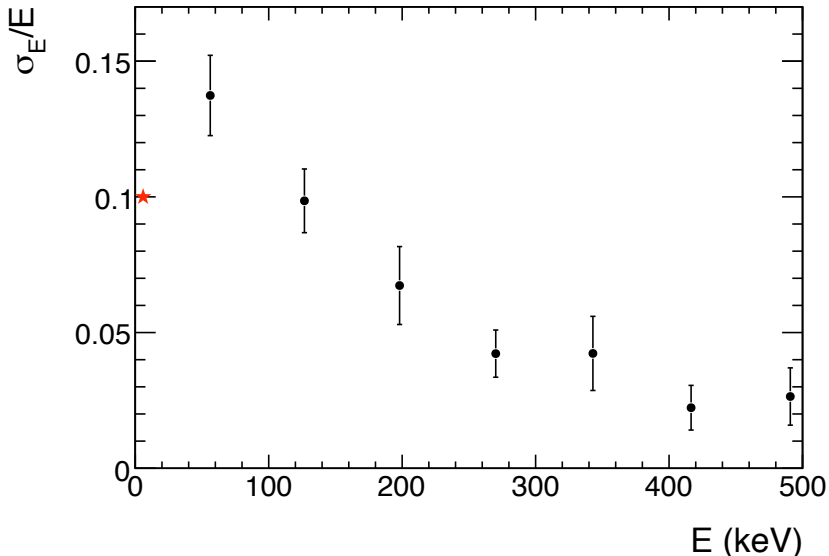


Fig. 2. Energy resolution measured with the charge and CCD readout. The star is the  $^{55}\text{Fe}$  peak from charge readout, and the remaining points are from the optical readout of tracks from the  $^{241}\text{Am}$  sources.

### 3 Measurement of $D/\mu$

Electrons propagating through  $\text{CF}_4$  gas experience a spread in transverse direction  $\sigma^2 \propto D/\mu$  where  $D$  is the diffusion constant and  $\mu$  is the mobility of electrons, i.e. a constant of proportionality between the drift velocity and the electric field. The  $D/\mu$  parameter is a measure of the average electron energy,  $\langle \varepsilon \rangle = \frac{3}{2} (D/\mu)$ .

In previous measurements of  $D/\mu$ , the spread of electron current was determined with annular anodes that integrate the swarm current [10,20] or with a small-area proportional counter that scans the swarm profile [8]. These approaches yield  $D/\mu$  values that differ by more than an order of magnitude at electric field to number density ratio  $E/N \sim 10 \text{ Td}^1$ . The large data samples of these measurements suggests that the discrepancy is due to an unknown systematic offset, which motivates a new measurement with a different approach.

In this work, we extract  $D/\mu$  from the width of alpha tracks ( $^{241}\text{Am}$ ) that are placed at different drift distances inside the drift cage. A 500 ms CCD exposure with alpha tracks emerging from the five sources is shown in Figure 3. The gaps in the tracks are the result of missing light due to the resistive separators which are used to maintain the amplification gap separation. Images are taken without a shutter, so it is possible that some alpha tracks appear during the CCD readout. Since the CCD is read out in a horizontal direction, these tracks appear shifted to the left or right. Most of such tracks fall out of the fitting range of interest or appear at wrong  $y$ -positions and can be excluded by requiring that the mean of the light distribution of the track segment agrees with the position of the source.

We collect 1000 images with 500 ms exposure for each  $E/N$  measurement point. The  $\text{CF}_4$  pressure is 50-150 Torr, and the temperature is roughly 300 K. In each track we select a 1.2 mm long segment taken 3 cm from a source and project it onto the  $y$ -axis. The projection is then fitted assuming a gaussian signal and a constant term for background, as shown in Figure 4. We compute the average width squared,  $\sigma^2$ , from the collection of all tracks from a single source that have a yield which is consistent with that of a single alpha track. The width squared is expected to change linearly with the drift distance,  $z$ , according to

$$\sigma^2(z) = \sigma_0^2 + 2 \left( \frac{D}{\mu} \right) \left( \frac{zL}{V} \right) \quad (1)$$

<sup>1</sup>  $1 \text{ Td} = 10^{-17} \text{V cm}^2$

where  $V$  is the applied voltage in the drift cage of length  $L$ . The detector resolution,  $\sigma_0$ , and  $(D/\mu)$  are free parameters that are determined in a fit to measurement points taken at five different drift distances and plotted in Figure 5.

Data points are taken at three different pressures (50, 75 and 150 Torr) and various drift voltages (1-5 kV). In regions where  $E/N$  values overlap, measurements are averaged in 1 Td bins of  $E/N$ . Results are shown in Figure 6 and listed in Table 1.

The dominant source of uncertainty is due to the choice of the position and size of the segments used in computation of the track widths. The dependence on the position of the segment is due to fringe fields in the drift cage that affect more strongly electrons that travel large drift distances. The percent error due to fringe field effects is larger for lower electric field values, as shown in Table 2. Also, increasing the length of the segment increases the width of the track due to imperfect collimation of the alpha sources. We also assign conservative errors by observing a difference in the  $D/\mu$  measurement after changing the pressure, the amplification voltage and the quality of focus at the same  $E/N$  value. Gas impurities are taken from the manufacturer's specification sheet (in ppm):  $O_2$  ( $< 2$ ),  $SF_6$  ( $< 1$ ),  $N_2$  ( $< 4$ ),  $CO$  ( $< 1$ ),  $CO_2$  ( $< 1$ ),  $H_2O$  ( $< 1$ ) and other fluorocarbons ( $< 2$ ) [21]. We confirm that the measurement is immune to outgassing effects by repeating the measurement over several days and obtaining consistent results ( $\sim 1\%$ ) in both  $D/\mu$  and detector gain.

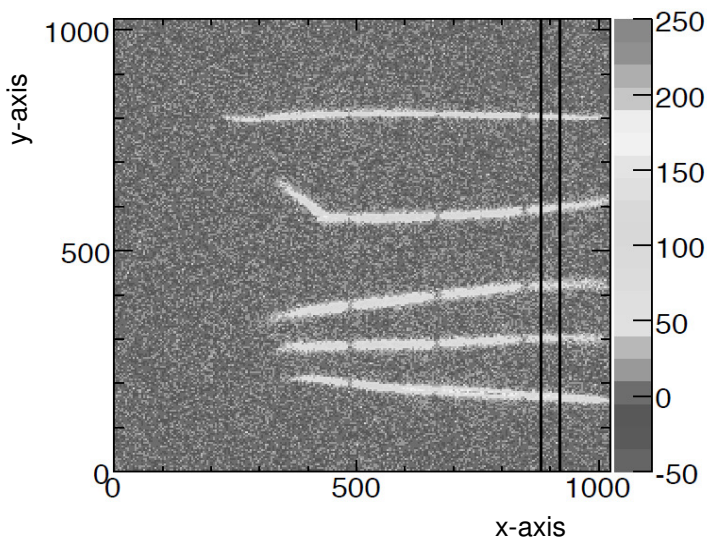


Fig. 3. A CCD image of 5 active sources of 5.4 MeV alpha particles. The viewfield is approximately  $14.4 \times 14.4 \text{ cm}^2$ . Vertical lines depict a 1.2 mm wide region of interest approximately 3 cm from the sources for measurement of track widths. The kink in the second track from the top is likely due to a large-angle scattering on gas nucleus.

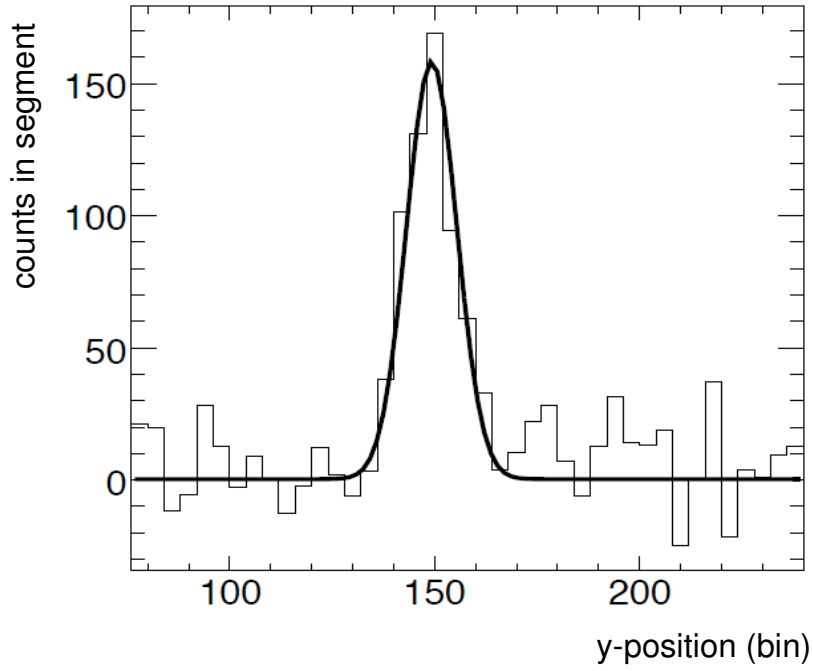


Fig. 4. A fit to the transverse profile of a track segment for a source at  $z = 9.1$  cm. 1 bin corresponds to  $143 \mu\text{m}$  in the image plane.

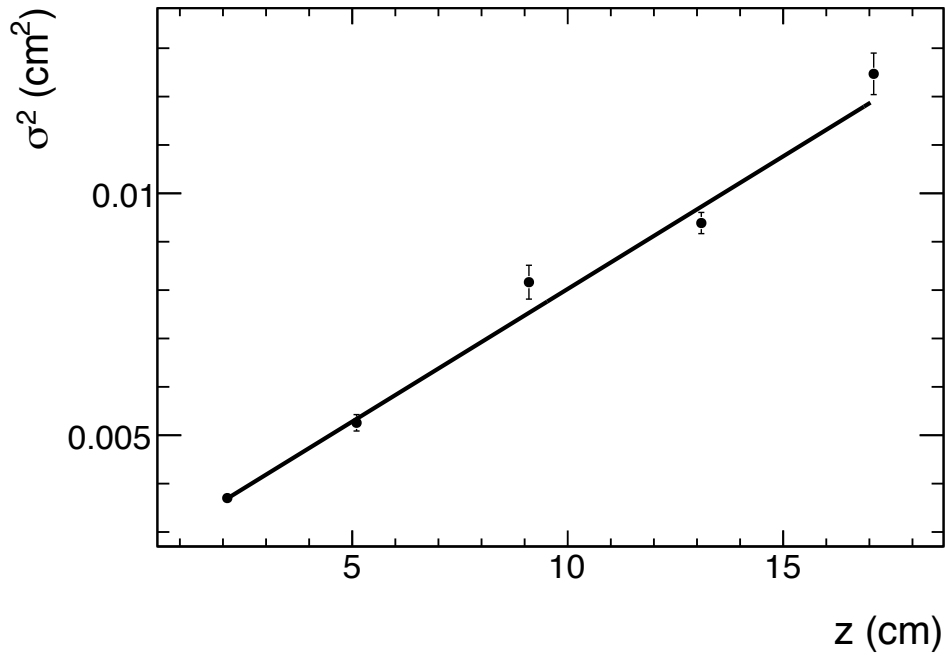


Fig. 5. Fit of a linear function to  $\sigma^2$  versus  $z$  for the  $E/N = 5$  Td data point.

Table 1

Measured values of  $D/\mu$ . Errors are dominated by systematic uncertainties that are listed in Table 2.

$E/N$ (Td)	$D/\mu$ (V)
1	0.027
2	0.027
3	0.032
4	0.033
5	0.033
6	0.039
7	0.037
8	0.042
9	0.044
10	0.051
11	0.055
12	0.055
13	0.062
14	0.078

#### 4 Attenuation coefficient

Attenuation of the signal in a gaseous detector is possible due to attachment of primary ionization electrons to  $\text{CF}_4$  molecules [1] and due to pollutants in the detector vessel. While attachment to impurities like oxygen can be minimized by evacuating the vessel before use and using a high-purity gas, attachment to molecules of the counting gas itself is unavoidable. Electron attachment leads to signal attenuation and degraded energy resolution. An understanding of the attachment rate is important, particularly for time-projection chambers with large drift distances. A signal with initial strength  $M_0$  will be attenuated to a strength  $M$  as a function of drift distance  $z$  according to

$$M = M_0 e^{(\alpha+\eta)z} \approx M_0 e^{\eta z} \quad (2)$$

where  $\alpha$  is the electron gain rate ( $\alpha \geq 0$ ) and  $\eta$  is the electron loss rate ( $\eta \leq 0$ ). We assume that the ionization rate  $\alpha$  is negligible [1] so we measure only the attenuation coefficient,  $\eta$ . Current measurements of  $\eta$ , have large discrepancies: for example, at  $E/N = 10$  Td, measurements of the loss of electrons after drifting 20 cm in 75 Torr of  $\text{CF}_4$  vary from 0% [11] to 70% [12];



Table 2

Summary of systematic errors for the  $D/\mu$  measurement. Contributions are added in quadrature to give the total.

Source	Error
Collimation, segment size and location	11% ( $E/N > 5$ Td)
	20% ( $E/N < 5$ Td)
Amplification voltage	8.9%
Quality of focusing	4.5%
Gas purity	5%
CCD readout noise	< 1%
Total	16% ( $E/N > 5$ Td)
	23% ( $E/N < 5$ Td)

possibly due to an unknown systematic offset.

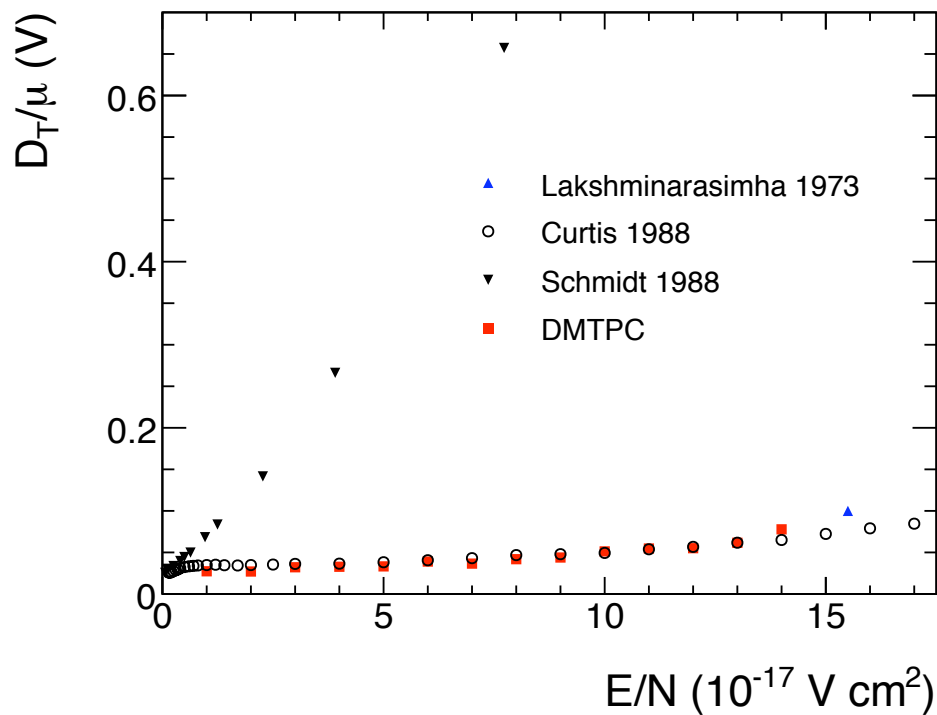


Fig. 6. Measured values of  $D/\mu$  as a function of  $E/N$  compared with other measurements.

Table 3

Measured values of attenuation coefficient in  $\text{CF}_4$  gas. Systematic errors are estimated to be less than 3%.

$E/N$ (Td)	$\eta/N \pm \text{stat}$ ( $\times 10^{18} \text{ cm}^2$ )
5.5	$-0.00026 \pm 0.00006$
10.6	$0.00027 \pm 0.0001$

We measure the attachment coefficient by placing a collimated  $^{55}\text{Fe}$  source at different heights and recording total charge collected at the anode. The source is located at the edge of the drift volume and placed on a cage ring directed radially toward the center of the TPC. We collect data for 250 sec with an  $^{55}\text{Fe}$  source and 1000 s without any source. Distributions of pulse heights taken with  $^{55}\text{Fe}$  positioned 2.1 cm from the anode and without any source are shown in the same plot in Figure 7; both taken at +730 V on the anode and -2600 V on the drift electrode. In all plots the background distribution is scaled to 250 sec. In a background-subtracted distribution that is shown in the same figure, we can clearly identify a 5.9 keV full absorption peak and a smaller, wider escape peak from the same X-ray line, and we can then describe the distribution with two Gaussians. The procedure is repeated for different drift heights and voltages. The attenuation coefficient,  $\eta$  in Equation (2), is extracted by varying the drift height  $z$  and making measurements of the position of the full absorption peak. Attenuation parameters at two different values of  $E/N$  are listed in Table 3. We compare this result with previous measurements in Figure 8, and we find that our result is consistent with zero and values from Ref [11], but inconsistent with the values from [12].

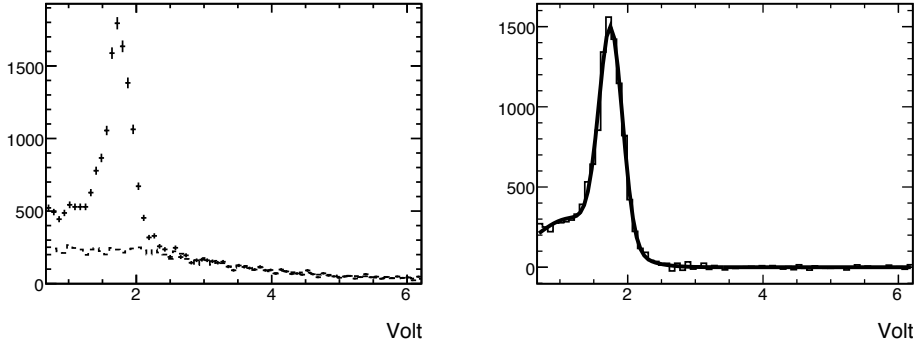


Fig. 7. Distribution of pulse heights with an Fe-55 source and without a source (left). Fit to the background-subtracted distribution (right).

The reported value of  $\eta/N$  is affected by the uncertainty of the pressure gauge (2%) and the temperature sensor (2%). We make measurements within a few hours of a new fill with  $\text{CF}_4$  gas, so the effect of outgasing is expected to be small. This is corroborated with previously mentioned stability in  $D/\mu$  and detector gain over several days. We confirm that the uncertainty in the spectrum model has negligible impact on the attenuation measurement by

fitting the spectrum around the full-absorption peak with a single gaussian and observing a change in the peak position of less than 1%. We also neglect the error due to imperfect collimation of X-ray source, as this does not change the mean of the drift length. We add all systematic errors in quadrature.

## 5 Conclusion

We have measured the average energy ( $D/\mu$ ) and attenuation rate of electrons ( $\eta/N$ ) drifting in  $\text{CF}_4$  gas at operating conditions of low-pressure TPC's ( $E/N = 1 - 10$  Td). Discrepancies in previous measurements of these parameters are an obstacle in designing a large volume TPC that is required for high-sensitivity experiments, such as dark matter searches. Our measurement of the  $D/\mu$  parameter is done by imaging alpha tracks that are placed at different heights in the drift cage. The results are consistent with measurements in Ref. [9], but disagree with Ref. [8]. The imaging technique can be applied to measurements of  $D/\mu$  for other gases and mixtures that allow optical readout. The systematic errors can be reduced by improving detector uniformity and using smaller CCD pixel bins.

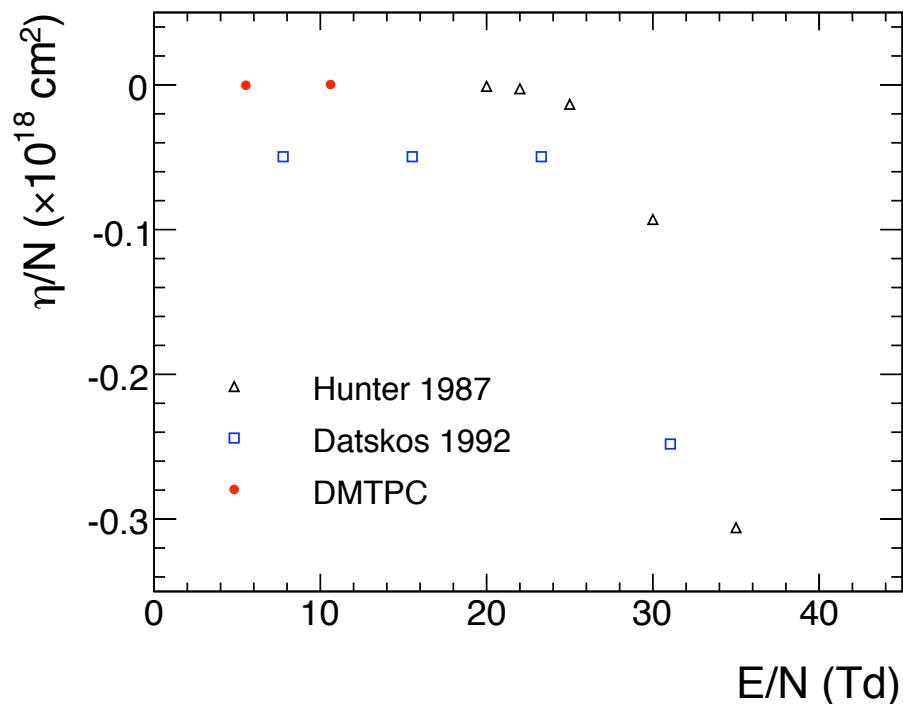


Fig. 8. Reduced attenuation coefficient ( $\eta/N$ ) as a function of reduced electric field ( $E/N$ ) compared with previous measurements.

The reduced attenuation coefficient ( $\eta/N$ ) is measured by collecting charge created by a collimated X-ray source that is placed at different drift heights. We find that the  $\eta/N$  is consistent with zero – a trend predicted by Ref. [11], but in disagreement with measurements in Ref. [12].

## References

- [1] L. G. Christophorou and J. K. Olthoff, *Fundamental Electron Interactions with Plasma Processing Gases*, Kluwer Academic/Plenum Publishers (2004).
- [2] D. N. Spergel, Phys. Rev. D **37**, 1353 (1988).
- [3] J. R. Ellis and R. A. Flores, Phys. Lett. B **263**, 259 (1991).
- [4] J. L. Vuilleumier, *Prepared for International Workshop on the Dark Side of the Universe: Experimental Efforts and Theoretical Framework*, Rome, Italy, 23-25 Jun 1993.
- [5] J. I. Collar and Y. Giomataris, Nucl. Instrum. Meth. A **471**, 254 (2000).
- [6] T. Tanimori, H. Kubo, K. Miuchi, T. Nagayoshi, R. Orito, A. Takada and A. Takeda, Phys. Lett. B **578**, 241 (2004).
- [7] D.R. Nygren, PEP-0144, Proceedings of PEP Summer Study, Berkeley 1975, 58-78.
- [8] B. Schmidt and S. Polenz, Nucl. Instr. Meth. A **273** (1988) 488.
- [9] M. G. Curtis, I. C. Walker, and K. J. Mathieson, J. Phys. D: Appl. Phys. **21** (1988) 1271-1274.
- [10] C. S. Lakshminarasimha, J. Lucas, and D. A. Price, Proc. IEE, **120**,9 (1973) 1044.
- [11] S. R. Hunter, J. G. Carter, and L. G. Christophorou, J. Chem. Phys. **86** (1987) 693.
- [12] P. G. Datskos, J. G. Carter, and L. G. Christophorou, J. Appl. Phys. **71** (1992) 15.
- [13] D. Dujmic *et al.*, [DMTPC Collaboration] Astropart. Phys. **30**, 58 (2008).
- [14] A. Pansky, A. Breskin, A. Buzulutskov, R. Chechik, V. Elkind and J. Va'vra, Nucl. Instrum. Meth. A **354**, 262 (1995).
- [15] A. Kaboth *et al.*, [DMTPC Collaboration] Nucl. Instrum. Meth. A **592**, 63 (2008).
- [16] S. F. Biagi, Nucl. Instrum. Meth. A **421** (1999) 234-240.
- [17] J. F. Ziegler, J. P. Biersack, and U. Littmark, Pergamon Press, New York, 1985. The code is available online at <http://www.SRIM.org>.

- [18] G. D. Alkhazov, Nucl. Instrum. Meth. **89**, 155 (1970).
- [19] M. S. Naidu and A. N. Prasad, J. Phys.D **5** (1972) 983.
- [20] L. G. Huxley and R. W. Crompton, *Diffusion and Drift of Electrons in Gases*, Wiley Series in Plasma Physics (1974).
- [21] Airgas spec. sheet for CF<sub>4</sub>; <http://www.airgas.com>.